AVO FEASIBILITY STUDY FOR HYDROCARBON DETECTION IN NORTHWESTERN PART OF THE PATTANI BASIN, GULF OF THAILAND

Kumhang Punglusamee

Petroleum Geocience Program, Department of Geology, Faculty of Science, Chulalongkorn University, Bangkok 10330, Thailand Corresponding author email: Kumhang2@gmail.com

Abstract

The Pattani Basin is one of the prolific areas for hydrocarbon exploration within the Gulf of Thailand. The main reservoirs of the area are Lower to Middle Miocene sands associated with fluvial depositional systems. Detection and quantification of hydrocarbon zones is not always accurate only by using conventional seismic amplitudes. I applied rock physics and AVO technique on one of the hydrocarbon fields of the northern Pattani Basin to understand AVO response for different fluids and for different reservoir thicknesses. According to rock physics analysis, P-impedance alone cannot successfully differentiate water-wet and gas saturated sands. However, used in conjunction with Poisson's ratio it can separate gas-saturated sands. Similarly, cross-plot of Lambda-Rho vs Mu-Rho can also separates gas-saturated zones. AVO modeling reveals that most of the gas sands are class-III sands. Some of the gas sands and water-wet sands deviate from general predicted trend. The possible reasons for these deviations are 1) thickness of sands is below tuning thickness 2) Shales with very low Poisson's ratio over sand reservoirs. According to wedge modeling results, gas sands below tuning thickness do not show typical class III response. Presence of very low Poisson's ratio shales above the sand reservoirs may affect AVO response as AVO depends upon contrast of Poisson's ratio. AVO attribute analysis indicates that scaled Poisson's ratio change is more suitable to detect gas sands within this area. The sands greater than tuning thickness can be detected more effectively by AVO attributes as compared to thin sands. Extracted horizon slices of scaled Poisson's ratio can provide useful information for promising exploration zones, if analyzed with structure contour maps.

Keywords: Pattani Basin, Rock Physics, AVO analysis

1. Introduction

AVO analysis is very popular tool to explain variation of seismic amplitudes in terms of rock properties and fluids (Avseth et al., 2005). In many places, this technique proved successful. In this study, an attempt has been made to apply AVO technique for the prediction of hydrocarbons in northwestern part of the Pattani Basin within the Gulf of Thailand. Different attempts have been made to study the relationship of bright amplitudes and AVO analysis in the Gulf of Thailand (Sukitprapanon, 2010 and Visadsri, 2013), but results were not encouraging to use AVO technique in the Gulf of Thailand. Therefore, it is required to understand the AVO response of different lithologies and different fluids to determine effective utilization and limitation of AVO technique in the GOT (Figure 1).

The detailed objective of the study can be summarized as below.

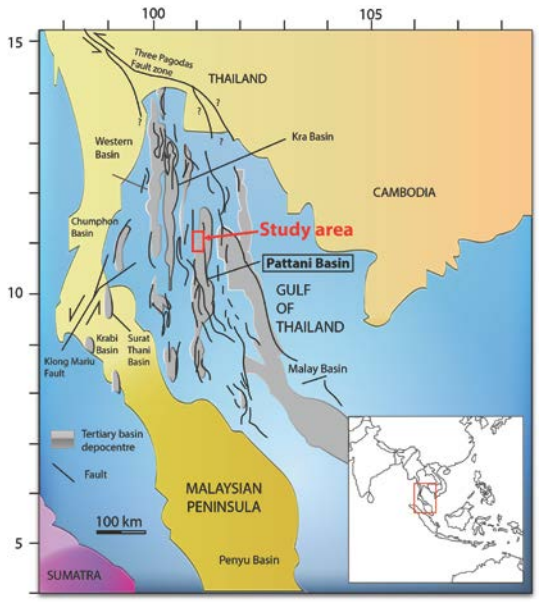

Figure 1. The regional map of the Gulf of Thailand. The highlighted red square is study area (modified form Morley and Racey, 2011)

1) Rock physics analysis to determine effective rock physics properties to differentiate lithologies and fluids.

2) Detail AVO modeling using well log data by creating AVO synthetic gather to study the AVO response in hydrocarbon saturated sands, brine sand and coal in order to identify different classes of AVO response in each case.

3) Perform tuning thickness analysis based on wedge model to study and understand the effect of reservoir thickness on AVO response.

4) To compute AVO attributes and to test them at well locations for different fluids.

5) Explain the limitation of the AVO technique in the study area.

2. Database and methodology

Conventional log data of six wells was available for present study. All wells have both P-wave and S-wave sonic logs. Moreover, full stack seismic data along with three partial angle stack volumes of near (5-22 degree), mid (18-35 degree) and far (36-60 degree) covering approximately 1200 sq.km of RIP field of the Pattani Basin.

Rock physics analysis

Cross-plot of P-velocity, S-velocity, Density, Vp/Vs, Poisson's ratio, P-impedance, S-impedance, Lambda*Rho and Mu Rho with respect to rock properties (color coded by depth, V-shale, porosity and water saturation) were used in order to determine which rock parameter that are appropriated for the lithology and hydrocarbon discrimination in this area. Also, the cross-plot analysis in this study were stratigraphically plotted (MMU to C, below C to K and below K to bottom hole) to see the variation of rock properties and physical rock properties that could change dramatically in different depth, sand properties and saturation within stratigraphic sequences. saturation sand. In this study, only some of selected cross-plots were chosen to show the relationship of rock physics.

AVO modelling and synthetic seismogram generation

Forward modelling of AVO response (by creating synthetic gathers) was carried out as feasibility study of hydrocarbon prediction before interpretation of real seismic data. The models were analyzed for characteristics of reservoir sand with fluid response. In this study, most of thick brine and hydrocarbon sands at different depth of six existing wells were modeled by using the Zoeppritz algorithm (Zoeppritz, 1919) with near stack wavelet along wellbore from 0–60 degree of both 1 ms and 4 ms sampling rate in order to compare with real seismic data (4 ms). Synthetic gathers in every case were analyzed by using AVO gradient analysis of two term Aki-Richards (Intercept (A)/Gradient (B)). The cross-plot of intercept and gradient from top and bottom sand were classified based on Classification chart of Castagna et al. (1998).

Synthetic seismograms were generated for six wells to tie well and seismic data. The wavelet used in this process is extracted wavelet along wells.

Tuning effect analysis based on wedge model

Tuning thickness in the study area was analyzed on the basis of wedge model (Widess, 1973) between 1300 to 2000 millisecond by using wavelet from each interval of full stack data. To further demonstrate the tuning effect, wedge models were generated along with pseudo logs of density, P-wave and S-wave for reservoir sand thickness ranging from 0-150 m. This model was convolved with wavelet to generate synthetic angle gathers for different thicknesses. Tuning thickness was assumed by determining maximum amplitude value due to construction interference.

AVO synthetic gathers of different thickness which is $\lambda/16$, $\lambda/8$, $3\lambda/16$, $\lambda/4$ and $5\lambda/16$ in accordance with Widess graphic formula were created to observe the thickness effect on AVO response. Two different extracted wavelets used for shallow and deeper

parts. The shallow part is defined from 1300 to 1600 ms, whereas deeper one is defined from 1700 to 2100 ms.

AVO attributes analysis based on 3D seismic

Range limited stacks of near (5-22) and mid (18-35) volumes were merged into single (N and M angel stack) volume which include near and mid angle trace showing in the same trace position. Then, the volume can be used to analyze cross-plot of intercept and gradient to identify lithology and hydrocarbon effect based on the possible relationship that derived from gradient analysis as in AVO modelling part. Different AVO attribute volumes can also be computed such as Intercept (A), Gradient (B), product A*B and Scaled Poisson's ratio change volume to predict lithology and hydrocarbons. Top of thick gas sand that shows bright spot in full stack were mapped in near and mid volume to show the amplitude variation with offset. Moreover, top of selected sands were mapped in near and mid stack volume to produce cross-plot relationship of near and mid amplitude.

3. Results

Rock physics

Cross-plot analysis of P-impedance and GR color-coded by water saturation

Cross-plot analysis of P-impedance and GR of shallow and deep stratigraphic intervals. Figure 2A shows that in shallower sequence 4, P-impedance can discriminate sand and shale (Figure 5A), whereas in deeper sequence 2, P-impedance cannot clearly differentiate sand and shale (Figure 2B). Gas saturated sands show similar P-impedance as of water-wet sands at all levels (Figure 2A and 2B).

Based on cross-plot analysis we can infer that P-impedance can only discriminate lithology in shallower zone. Moreover, gas saturated zones cannot be separated by using P-Impedance alone.

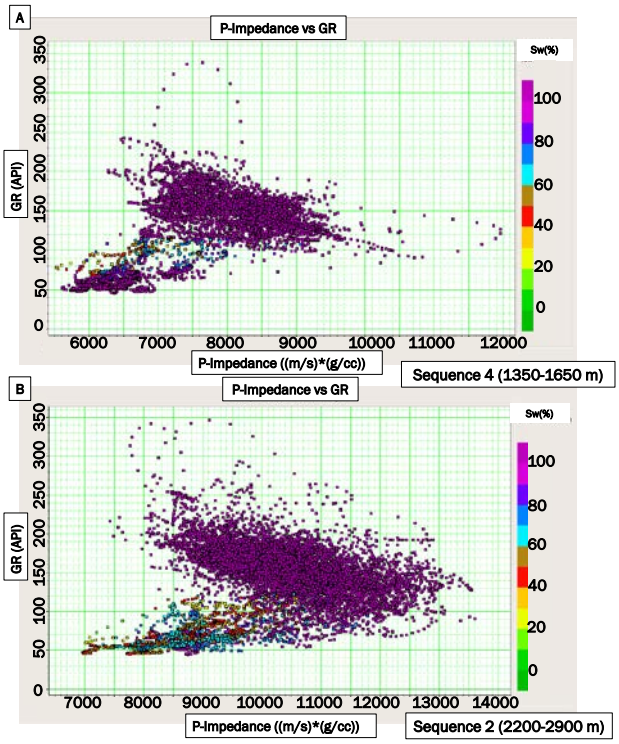

Figure 2. Cross-plot of P-impedance and GR color-coded by water saturation in well #2 A) within sequence 4 (1350-1650 m) B) within sequence 2 (2200-2900 m). Sands have lower P-impedance for shallow sequence, but in deeper levels, sand and shale have relatively same P-impedance.

Cross-plot analysis of P-impedance vs. Poisson's ratio with respect to lithology and reservoir fluids

The cross-plot of P-impedance and Poisson's ratio color-coded by clay volume shows that sands have low P-impedance and Poisson's ratio (Figure 3). Sands have generally low Poisson's ratio marked by yellow circle in Figure 3. The values of Poisson's ratio in sands range from 0.5 to 0.25. According to the cross-plot of P-impedance and Poisson's ratio color-coded by water saturation within stratigraphic interval of sequence 3 (Figure 4), gas saturated sands (within red circle) have very low Poisson's ratio as compared to water saturated sands (Figure 4).

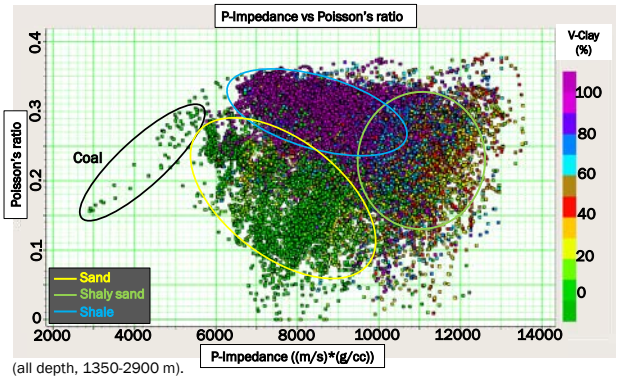

Figure 3. Cross-plot of P-impedance vs. Poisson's ratio color-coded by clay volume in well #2 (all depth, 1350-2900 m) shows highlighted lithologies of sand, shaly sand, shale and coal.

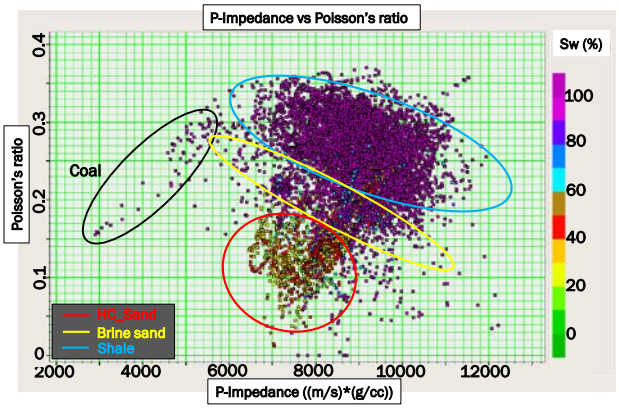

Figure 4. Cross-plot of P-impedance vs. Poisson's ratio color coded by water saturation in well #2 (Sequence 3-main pay window (1650-2200 m)). Hydrocarbon saturated zone give lower Poisson's ratio as compared to brine sand.

Some points on cross-plot show low Poisson's ratio in the range of Poisson's ratio of gas-saturated sands, but have relatively high P-impedance. Figure 5 reveals that these are shale points, having low Poisson's ratio (highlighted by red polygon). This characteristic is different from dominant shale sequences in the Gulf of Thailand, which generally shows high Poisson's ratio. This shale has higher P-impedance than sand (9000-10000 m/s*g/cc) and give similar Poisson's ratio as of gas saturated sands (0.05-0.15). On the other hand coal beds show very lower impedance (3000-6000 m/s*g/cc) and moderate Poisson's ratio (0.15-0.3) (Figure 3). These coal beds have low density values (less than 2 g/cc), moderate gamma ray (130-200 API) and high transit time (340-380 msec/m). These coal beds have pervasively distributed in sequence 3. According to core analysis (Jirach, 2013), it could be non-marine coals situated in sequence 3.

Based on cross-plot analysis P-impedance and Poisson's ratio in combination can discriminate lithology and gas saturated zones in the area. P-impedance and Poisson's ratio are better discriminator of lithology and reservoir fluids. However, it has to realize that the AVO response is depending on the Poisson's ratio contrast of the rock layer (Castagna and Smith, 1994). Thus, low Poisson's ratio shale that distributed throughout this area can give false anomalies of gas sands.

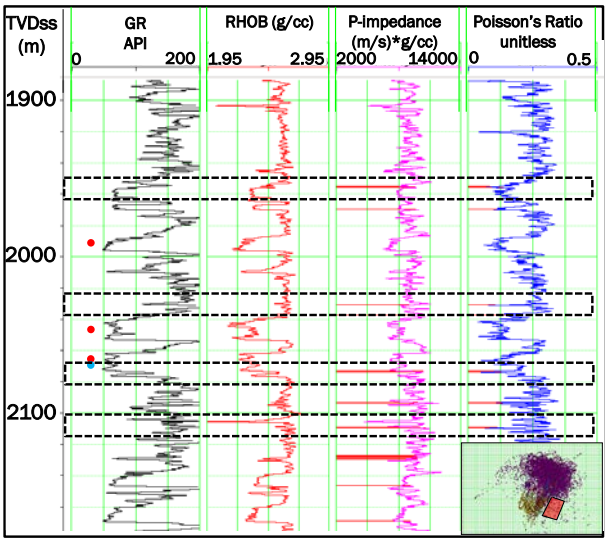

Figure 5. Low Poisson's ratio shale response in the cross-plot of P-impedance vs. Poisson's ratio color-coded by water saturation and log section in well #2 (sequence 3 (1650 -2200 m)). Red highlighted low Poisson's ratio zone in cross-plot is shaded red in log section.

AVO modeling

In this study, number of gas, oil and brine sands in six wells at different depth zones

were modeled for AVO analysis. Figure 6 show typical AVO and log response of gas sand (at 1738 ms, 2040 m) within a representative well in the study area. Gradient curves show that most of the top gas sands are of negative amplitude at zero offset and amplitudes become more negative with offset gas saturated sands whereas the deeper oil reservoir (at 1863 ms, 2350 m) within sequence 2 behave like water wet sand. Mixed phase hydrocarbon sand such as thin net pay of gas on water, oil on water and gas on oil show relatively low gradient (Figure 7). Moreover, the AVO response of coal was also studied

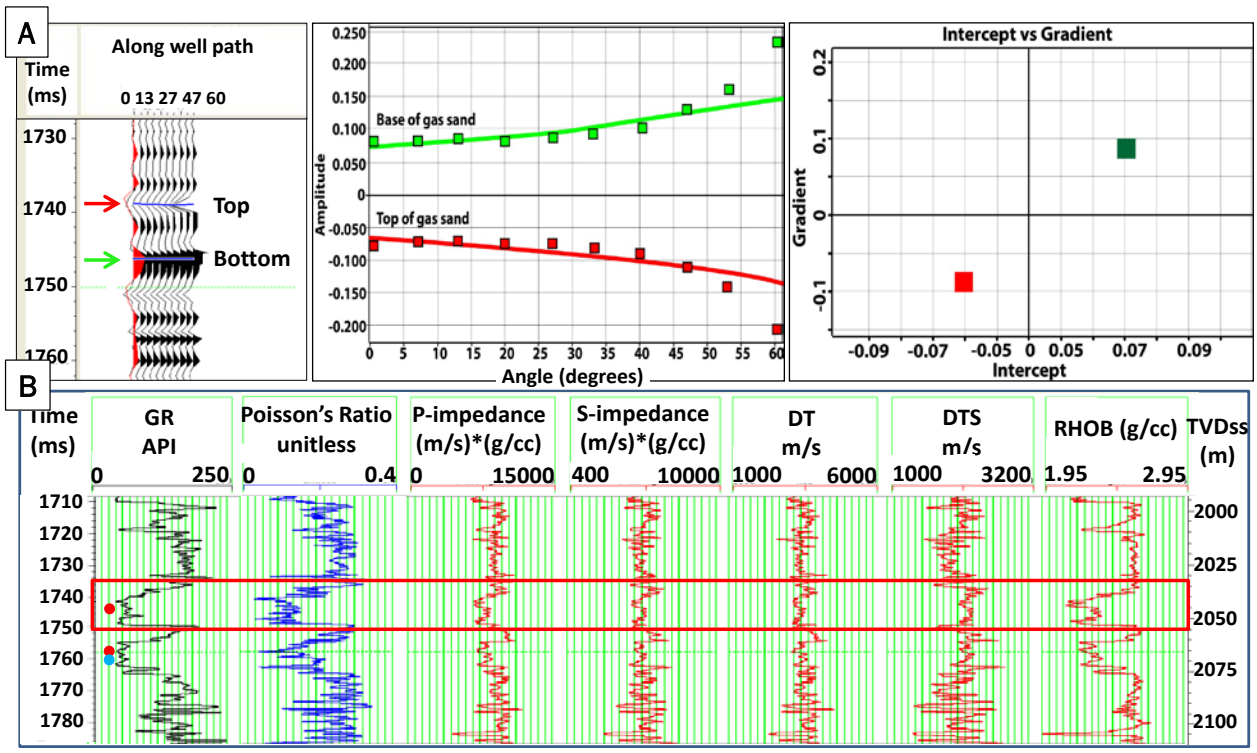

Figure 6. A) Typical AVO response gas sand (at 1738 ms of well #2) B) general log response for gas sand.

on synthetic gather. The base of gas sand is characterized by positive amplitude, which slightly increases with angle (Figure 6). In the case of top of brine sands, negative amplitudes become less negative and changes to positive at high angle.

Figure 7 shows gradient intercept cross plot of different sands with different fluids such as gas, oil, brine, gas on oil and gas on water in six wells within the study area. Top and base of gas sands in all wells mostly situated in quadrant III and I on intercept gradient cross plot respectively. For water sands, top and bottom mostly situated in quadrant II and IV. There are only two oil reservoirs (Figure 7) in well #4 and #6. Oil sand (at 1304 ms, 1371 m) in the shallower part within sequence 4 has AVO response similar to (Figure 8). It shows different AVO response from gas sands. The top of coal behave the same as of brine sand but gives relatively higher intercept (Figure 6A and 8). Therefore, very bright amplitudes due to the presence of coals can be discriminated from anomalies of gas-saturated sands based on AVO analysis. Figure 7 reveals that in some cases AVO response of gas sands and water-wet sands deviates from the general observed trend. For example, on the Intercept-gradient cross plot (Figure 9B), gas sand (at 1678 ms) in well #3 which is 19.81 m, thick and has 46% water saturation shows top AVO response at very low positive gradient in quadrant III of AVO cross-plot. At the top of this gas, sand very low Poisson's ratio shales are situated (Figure 9A). The low Poisson's ratio of this shale can

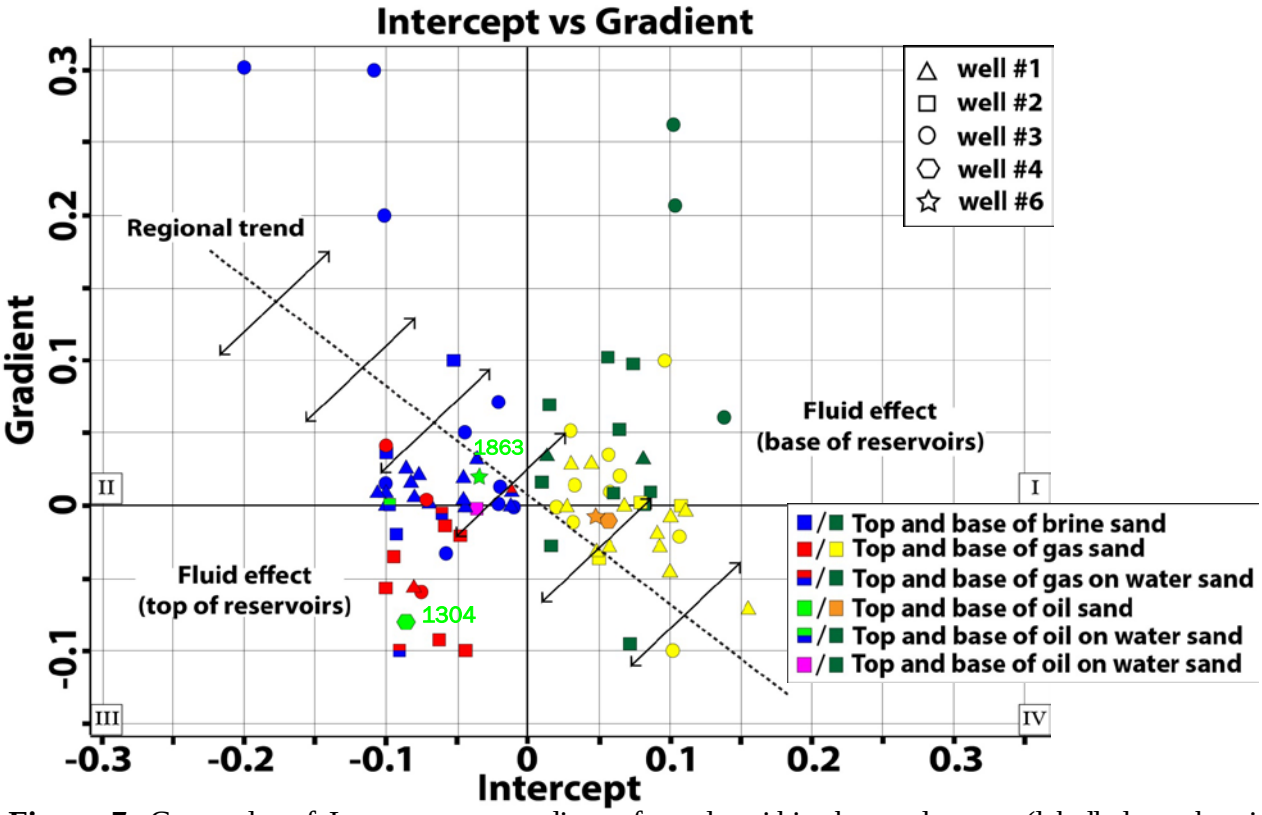

Figure 7. Cross-plot of Intercept vs. gradient of sands within the study area (labelled number is top of sand (ms)) and an interpretation of general relationship of AVO response in the area.

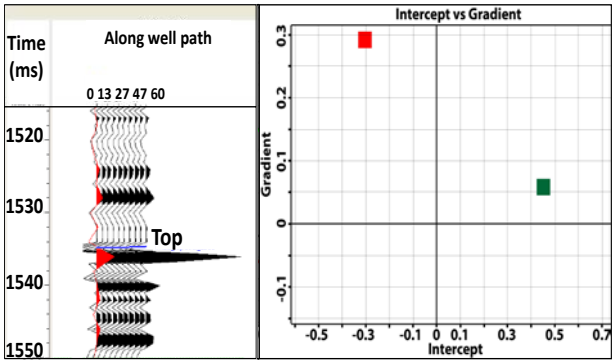

Figure 8. Synthetic gather and amplitude variation with offset angle along with cross-plot of Intercept and gradient in the case of coal bed

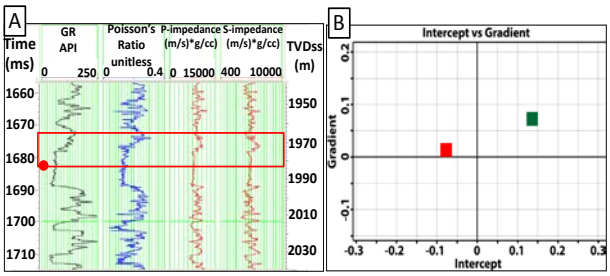

Figure 9. A) Very low Poisson's ratio shale at the top of gas sand reservoir (at 1678 ms of well #3). B) Intercept and Gradient cross-plot of the gas sand showing top response at quadrant II. It has very low positive gradient which may cause by low Poisson's ratio shale.

interfere with the AVO response. Figure 10B shows cross-plot of intercept and gradient of water wet sand (at 1562 ms, 1770 m) in well #3. This shows response like low gradient class III gas sands. In log section (Figure 10A), this water sand has lower Poisson's ratio as compared to general water wet sands and 90% water saturation. Therefore, small amount of gas in reservoir can give class III AVO sand.

According to modeling feasibility analysis, the lithology can be distinguished based on intercept values. All top sands are having negative intercept. Fluids within sands can be differentiated by gradient. Top of gas sands has negative gradient whereas top of brine sand has positive gradient. The gas sands in this area are interpreted as AVO class III sands (Castagana et al., 1998). Most of gas

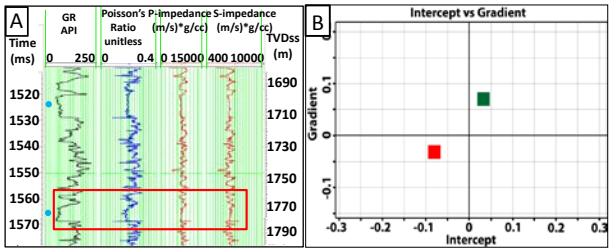

Figure 10. Wet sand in Well #3 that shows AVO response similar to gas sand. This brine sand has water saturation 90% and low Poisson ratio as compare to brine sand above so that it may be due to Fizz effect.

sands and water-wet sands show different AVO response (Figure 7). Therefore, gas saturated sands and brine saturated sands can be discriminated based on their AVO responses. Sometimes, very low percentage of gas saturation show similar response as of high percentage of gas saturation. Furthermore, in Pattani Basin, there are a lot of coals deposited within the main hydrocarbon zone interval (sequence 3) and may induce bright spot anomaly due to low acoustic impedance, but AVO technique can differentiate coal and gas because coals show different AVO response. However, there are low Poisson's ratio shales that are situated on top of the reservoir sands and they may generate false anomaly. In addition, Gas sand labeled 1710 in Figure 7 has the same response as top of brine sand because it is quite thin (4.9 m). This phenomenon will be discussed in the next section.

Tuning thickness analysis

Wedge model for shallow interval (1300 ms-1600 ms) and deep interval (1700 ms-2100 ms) were generated to compute the average tuning thickness in different zones by using specific extracted wavelet for each interval. Pick analysis chart shows the maximum amplitude (maximum constructive interference) at a 10 m and 24 m in shallow and deeper sections respectively. To further demonstrate offset-dependent tuning in the area, the effect of formation thickness on AVO characteristic has been studied by changing the thickness of AVO class III gas sand at deeper interval (Figure 11). In this analysis, I used the wavelength based on the deeper section interval (λ=96 m). The AVO responses of ratio λ/16, λ/8, 3λ/16, λ/4 and 5λ/16 (6, 12, 18, 24, and 30 m) in accordance with Widess graphic formula (Widess, 1973) are plotted and shown in Figure 11. A significant decrease in gradient can be seen when thickness of sand change from λ/4 to λ/16. In the case of very thin beds of λ/16 (6 m) the AVO response of top gas sand is like water wet sand. This illustrates that AVO analysis performed on thin (below tuning thickness) beds may not represent true fluid response.

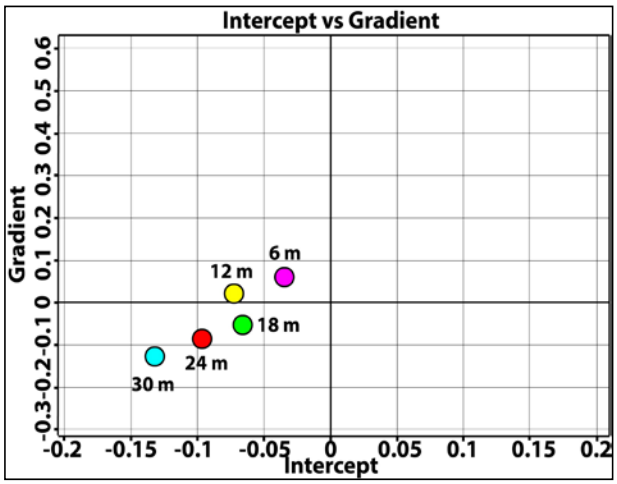

Figure 11. AVO responses for different thicknesses of sand reservoirs. Gradient decreases with decrease in thickness of reservoirs.

In this area, many sands are in the range of 4 to 20 meters thickness in middle and lower part (sequence 2 and 3). Therefore, it is not possible to get accurate AVO response for sands less than tuning thickness (24 m) in the deeper sections. However, in the shallow section, where tuning thickness is 10 m, we can get accurate AVO response for the relatively thinner beds.

AVO analysis based on seismic data

To analyze AVO response from actual seismic data, gas sands of different wells were analyzed and in the following section, key gas sands are discussed. Figure 12A and 12B show the result of gradient analysis of partial angle

stacks (near and mid volumes) of two gas sands at well #2 (at 1738 ms, 2040 m) and #3 (at 1678 ms, 1975 m). These selected gas sands are the same, which were modeled for AVO analysis and discussed in previous section (Figure 6 and 9). Both of these gas sands show similar results as it was exhibited in the AVO modeling. Figure 12A shows normal class III AVO trend of gas sand but Figure 12B shows the AVO response of gas sand (at 1678 ms, 1975 m) which has very low positive gradient for top gas sand.

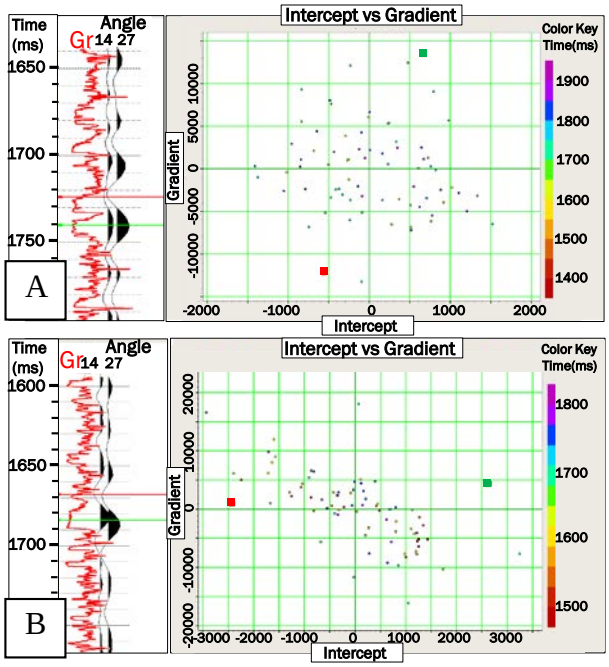

Figure 12. A) Intercept and gradient cross-plot of gas sand (at 1738 ms of well #2). B) Intercept and gradient cross-plot of gas sand (at 1678 ms of well #3).

Gradient intercept cross-plot of seismic data within 100 ms window centered at top gas sand show that the points plotted in quadrant III and I represent top gas sand and base of gas sand respectively on seismic section (Figure 13A and 13B). These zones are different from wet trend (grey polygon). The other selected gas sand of well #3 does not show distinguishable gradient intercept for top gas sand. In this case, small positive gradient is observed for top gas sand, which is similar to wet trend (Figure 12B). The same result was obtained in the case of AVO modeling of this gas sand (Figure 9).

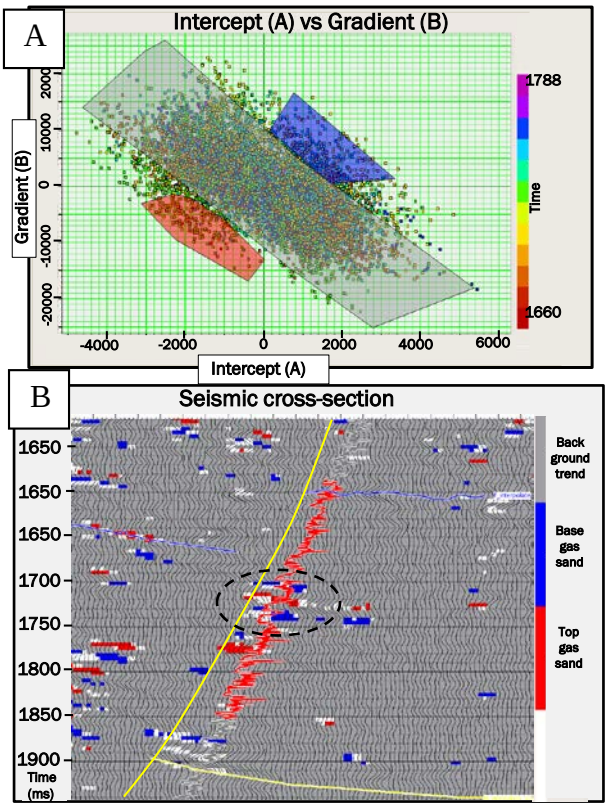

Figure 13. A) Intercept-gradient cross-plot of top gas sand horizon (at 1738 ms of well #3), using window interval of +/-100 ms. Highlighted zone in cross-plot is shown in B) near stack seismic section.

AVO attributes volume analysis

Two attribute volumes of scaled Poisson's ratio change (aA+bB) and product of intercept (A) and gradient (B) attribute were generated from near and mid angle partial stacks. Figures 14A-C shows three seismic sections of full stack seismic, scales Poisson's ratio change attribute and product A*B attribute volume along well #2. In this figure (yellow polygon), 15 meter thick gas sand (at 1738 ms, 2040 m) is very close to the top of the 14 meter gas on water sand (at 1750 ms, 2063 m), so both gas sands could be detected as only one thick gas sand on seismic resolution. This gas sand shows bright amplitude anomaly on full stack seismic data (Figure 14A). Scaled Poisson's ratio change attribute section (Figure

14B) shows a negative response (a decreasing in σ) at the top of reservoir (red arrow) and a positive response at the base (an increase in σ) indicating hydrocarbon-charged sand. Top and base of this gas sand show both positive value in Product A*B attribute section (Figure 14C). This represent typical class III AVO sand anomaly. There is another bright amplitude anomaly at 1880 ms (red arrow, Figure 14A). This anomaly is in between two thin gas sands, which are below tuning thickness. This anomaly is not visible on scaled Poisson's ratio change attribute. AVO attribute cannot detect these gas sands because of thinner reservoirs. Apparent bright amplitude on seismic section is may be due to constructive interference. Figures 15A-C shows AVO attributes response of 20 meter thick gas sand (at 1678 ms of well #3), which did not exhibit typical class III AVO response in modeling (Figure 9). This gas sand showed low positive gradient for the top of gas sands (Figure 9 and 12B). In this case product attributes for A and B does not show typical class III AVO positive response (Figure 15C) but scaled Poisson's ratio show negative Poisson's ratio at the top of the reservoir (Figure 15B). Therefore, scaled Poisson's ratio may work more effectively for different types of gas sand response in the area. Based on AVO attribute analysis and AVO modeling it can be concluded that AVO attributes such as Poisson's ratio and product of Gradient Intercept cannot effectively detect sands of thickness less than tuning thickness.

According to AVO attribute analysis, scaled Poisson's ratio is more suitable for detecting gas sands. Therefore, extraction of Poisson's ratio attribute along horizon slice may provide useful information for lateral distribution of gas-saturated zones. I also computed average anomaly map within pay zone (between C and F marker). This represents high average anomalies within the pay interval. The high anomalies are within faulted zone (Figure 16). Therefore, AVO attributes such as Poisson's ratio may provide information for gas saturated zone in the study area.

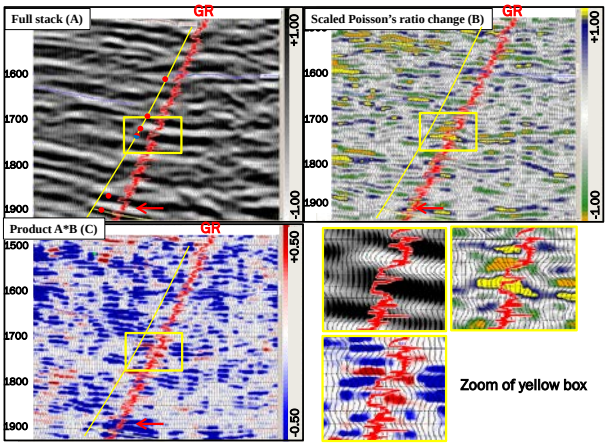

Figure 14. A) full stack seismic section, B) scale Poisson's ratio change and C) product A*B along well #2.

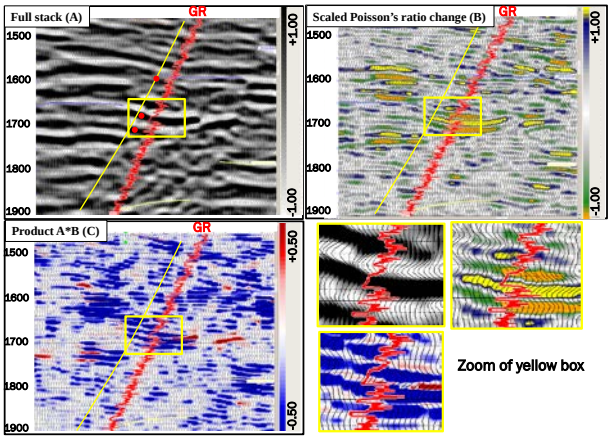

Figure 15. A) full stack seismic section, B) scale Poisson's ratio change and C) product A*B along well #3.

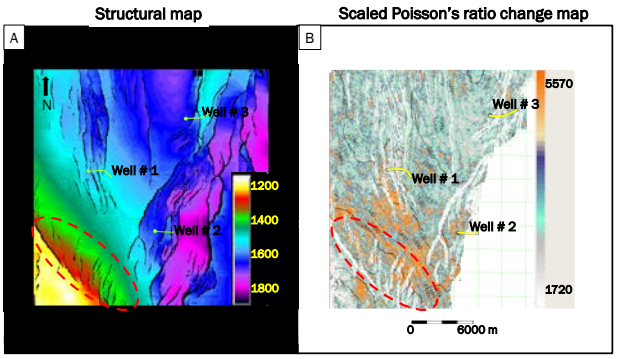

Figure 16 A) structural map of F horizon. B) Scaled Poisson's ratio change attribute from C to F horizon (main pay zone). Red zone in attribute map shows more possible stack hydrocarbon saturated sands.

Comparison with other basins

Gulf of Mexico

In the Gulf of Mexico, Rock physics analysis by Per Avseth and Ran Bachrach (2008) shows combination of Vp/Vs and P-impedance can discriminate lithology and fluids of shallow turbidite reservoir sands. The AVO results are similar to AVO response of this study. Gas sands of Gulf of Mexico also show typical class-III response for under compacted and unconsolidated plio-pliestocene turbidite sands (Rutherford and William, 1989). Gas sands in the Gulf of Mexico have average thickness in excess of 30 m and mostly associated with bright spot on full stack data. However, the fluvial sands in the Gulf of Thailand are relatively thinner and affected by tuning phenomena. Rutherford and William (1989) also observed deviation from class III anomalies due to tuning thickness effect.

Malay Basin

The Malay basin is situated in the southern part of the Gulf of Thailand. The reservoir interval consists of a vertical succession of over 2000 m of Early Miocene clay rich sediments deposited in fluvial to tidal estuarine and shallow marine settings (Barr et al., 2011). Across the succession, the depositional setting fluctuated between fluvial and tidal to shallow marine, with coals and carbonate more common in the deeper reservoir zones. However, in the area, rock properties vary with depth and in the shallow section good quality gas sands are acoustically soft compared to the surrounding shales, typically displaying low density and medium P-wave velocity for a combined low acoustic impedance log response. In addition, the Vp/Vs or Poisson's Ratio is low (Michel et al., 2011) but the contrast of these rock physics parameters are relatively less as compared to the Pattani Basin. The deeper sands are harder and mixed with more coal and carbonaceous shale. AVO responses in this area are generally class II gas sands (Castagna, 1997) which has very low negative intercept and negative amplitude in the shallow part and become AVO class I in the deeper part due to more compaction of sands (Ghosh et al., 2010). Although, basin development process is almost the same for the Pattani and Malay basins, yet AVO response for gas sands is different. This difference may be due to high percentage of carbonaceous material. Malay Basin has also the same problem of thin beds as it has fluvial and tidal dominated system. The average thickness of oil and gas pay zones in the Malay Basin is 10 m or thinner (Ghosh et al., 2010). Therefore, AVO technique may not be able to detect all sands of fluvial depositional environment. AVO can only detect thick fluvial sands. Tuning phenomena may also affect AVO responses of gas sands of other Tertiary rift basins of SE Asia.

Conclusion

The rock physics and AVO analysis were applied on a data of hydrocarbon field in northwestern Pattani Basin of the Gulf of Thailand. The main findings and conclusions are summarized below.

Rock physics analysis

Rock physics parameters such as Poisson's ratio vs. P-impedance, are useful to discriminate lithology and fluids.

Cross plot between Poisson's ratio vs. P-impedance shows that some shales have low Poisson's ratio similar to gas-saturated zones. These shales may give false AVO anomalies.

AVO modeling

Gas sands generally exhibit AVO class III anomalies. Top of gas sands show negative amplitude and become more negative with increasing offset.

Most of two phases hydrocarbon saturation sands have very low negative gradient.

Bright amplitudes, which are caused by thick coal beds show different AVO response. Coal beds show different AVO response as compared to gas sand (much higher intercept and has positive gradient).

Low Poisson's ratio shales on the top of gas sands may reduce the Poisson's ratio contrast and give low gradients.

Tuning thickness analysis suggests that AVO response is reduced in the case of thin gas sands.

AVO analysis of actual seismic data and AVO attribute volume

AVO response in the area can be detected only if the hydrocarbon charged reservoirs are thicker than tuning thickness.

Thick gas sand in well #3 (at 1678) shows AVO response like water wet trend because it has low Poisson's shale on the top of it. This response may be generated due to less contrast of Poisson's ratio between gas-saturated zone and overlying shale.

Scaled Poisson's ratio change is the most effective attribute.

Horizon slices of AVO scaled Poisson's ratio show anomalies along faults. These anomalies within structure closure may be promising zones for future exploration.

Future recommendations

Core data is required to understand the nature of low Poisson's ratio shales.

In order to perform fluid replacement rock properties such as gas density, young modulus and bulk modulus are required.

Angle gathers may give improved AVO analysis as compared to three partial angle stacks.

Acknowledgements

I would like to thank Chulalongkorn University for giving opportunity to pursue the master degree in petroleum geosciences and I would like to express my sincere gratitude to the program sponsors, Chevron Thailand Exploration and Production, Ltd. for the full scholarship for this program. Also, I would like to thanks my university supervisor professors Dr. Mirza Naseer Ahmad for final research project supervision and manuscript revision, and for Prof. Phillip Rowell and Prof. John K. Warren for the discussion during final research and knowledge during study time. Moreover, I also would like to thank Prof. Joseph Lambiase, Mr. Chris Morley and Dr. Punya Charusirifor their knowledge through the Petroleum Geoscience Program. I would like to thanks to Chevron staff especially Mr. Lance Brunsvold, Mr. Jim Logan, Mr. George Livesay and Mr. Sarayoot Geena who have provided valuable support and technical discussion. In addition, I am thankful to the CGG Veritas and Landmark graphics corporation for the donation of the software for this research project. Finally, I would like to acknowledge my friends and my family who supported me during my time here.

Reference

Aki, K., and P.G. Richards, 1980, Quantitative Seismology, first edition: San Francisco, W.H. Freeman and Company, 557 p.

Avseth, P., T. Mukerji, and G. Mavko, 2005, Rock physics depth trends and anomalies in a North Sea field, Quantitative Seismic Interpretation: Cambridge, Cambridge University Press, p. 96-101.

Bachrach, R., and Avseth, P., 2008, Rock physics modeling of unconsolidated sands: Accounting for nonuniform contacts and heterogeneous stress fields in the effective media approximation with applications to hydrocarbon exploration: Geophysics, v. 73, no. 6, p. 197-209, doi 10.1190/1.2985821.

Barr, D.C., M.J., Flynn, C.S., Ong and K., Dhamarajan, 2011, Interpreting Geological Systems from Seismic Attributes: Reasons for Caution from the Northern Malay Basin: ITPC 14830, 2011 International Petroleum Technology Conference, 15-17 November, Bangkok, Thailand.

Castagna, J.P., and Smith, S.W., 1994, Comparison of AVO indicators A modeling study: Geophysics, v. 59, no. 12, p. 1849-1855, doi 10.1190/1.1443572.

Castagna, J.P., and Swan, H.W., 1997, Principles of AVO crossplotting:

The Leading Edge, v. 16, no. 4, p. 337-344, doi 10.1190/1.1437626.

Castagna, J.P., Swan, H.W., and Foster, D. J., 1998, Framework for AVO gradient and intercept interpretation: Geophysics, v. 63, no. 3, p. 948-956, doi 10.1190/1.1444406.

Ghosh, D.M., Firdaus, A.H., Martin, B., Bernato, V., and Nasir, D., 2010, Geophysical issues and challenges in Malay and adjacent basins from an E & P perspective: The Leading Edge, v. 29, no. 4, p. 436-449, doi 10.1190/1.3378307.

Kamvan, J., 2013, Different types of organic-rich geological markers in the sub-surface in the North Pailin field, Pattani basin, Gulf of Thailand, Master's thesis, Chulalongkorn University, Thailand, 51 p.

Michel, L., H.H., Chee, R., Hampson, M.J., Flynn, H., Carigali, 2011, Application of PSDM Imaging for Reservoir Characterisation in the Northern Malay Basin: A Case Study: ITPC 1481, 2011 International Petroleum Technology Conference, 15-17 November, Bangkok, Thailand.

Morley, C.K., and A. Racey, 2011, Petroleum Geology, in M.F. Ridd, A.J. Baeber and M.J. Crow, eds., The Geology of Thailand: London, Geological Society, p. 351-392.

Morley, C.K., and A. Racey, 2011, Tertiary stratigraphy, in M.F. Ridd, A.J. Baeber and M.J. Crow, eds., The Geology of Thailand: London, Geological Society, p. 223-272.

Rutherford, S.R., and Williams, R. H., 1989, Amplitude-versus-offset variations in gas sands: Geophysics, v. 54, no. 6, p. 680-688, doi 10.1190/1.1442696.

Sukitprapanon, P., 2010, The relationship between seismic amplitude, lithology and hydrocarbons in southern RIP block, Gulf of Thailand, Master's thesis, Chulalongkorn University, Thailand, 141p.

Visadsri, P., 2013, Prediction of reservoir or sands by using rock physics and simultaneous inversion: Case study from the Pattani Basin, Gulf of Thailand, Master's thesis, Chulalongkorn University, Thailand, 136 p.

Widess, M.B., 1973, How thin is a thin bed?: Geophysics, v. 38, p. 1176-1180.

Zoeppritz, K., 1919, Erdbedbnwellen VIIIB, on the reflection and propagation of seismic wave: Gottinger Nachrichten, v. 1, p. 66-84.